Articles in PresS. Am J Physiol Lung Cell Mol Physiol (June 25, 2004). 10.1152/ajplung.00184.2003

Evidence for a role of Heat shock factor 1 in the inhibition of NF-κB pathway during the heat shock response-mediated lung protection

Delphine Wirth[1], Fabrice Bureau[2], Dorothée Melotte[2], Elisabeth Christians[3], Pascal Gustin[1].

[1]Unit of Pharmacology, Pharmacotherapy and Toxicology, [2]Unit of Physiology; Department of Functional Sciences, Faculty of Veterinary Medicine, University of Liege, 4000 Liege, Belgium.

[3]Center of development biology, University Paul Sabatier - Toulouse 3, 31062 Toulouse, France.

Running head: HSF1 and NF-κB in lung protection

Corresponding author during production of the paper: D. Wirth Unit of Pharmacology, Pharmacotherapy and Toxicology; Department of Functional Sciences, Faculty of Veterinary Medicine, 20 (B41), Bd de Colonster, 4000 Liège, Belgium.

E-Mail: delphine.wirth@ulg.ac.be

Tel: +32 4 366-4175

Fax: +32 4 366-4176

Corresponding author and reprint requests (to be included in the final article): P. Gustin, Unit of Pharmacology, Pharmacotherapy and Toxicology; Department of Functional Sciences, Faculty of Veterinary Medicine, 20 (B41), Bd de Colonster, 4000 Liège, Belgium.

E-Mail: p.gustin@ulg.ac.be

Tel: +32 4 366-4170

Fax: +32 4 366-4176

Keywords: Knockout Mice; Cadmium; Heat-Shock Proteins; Granulocyte-Macrophage Colony-Stimulating Factor.

Abstract

Heat shock transcription factor HSF1 is recognized as a central component of the heat shock response, which protects against various harmful conditions. However, the mechanisms underlying the protection and the role of HSF1 in these mechanisms have not yet been clearly elucidated. Using HSF1 knockout mice (*Hsf1*$^{-/-}$), this study examined whether HS response-mediated lung protection involved an inhibition of the pro-inflammatory pathway via an interaction between HSF1 and NF-κB, in response to cadmium insult. The HSF1-dependent protective effect against intranasal instillation of cadmium (10 and 100 µg/mouse) was demonstrated by the higher protein content (1.2 and 1.4-fold), macrophage (1.6 and 1.9-fold) and neutrophil (2.6 and 1.8-fold) number in bronchoalveolar fluids, higher lung wet-to-dry weight ratio, and more severe lung damage evaluated by histopathology in *Hsf1*$^{-/-}$, compared with wild-type animals. These responses were associated with higher granulocyte-macrophage colony-stimulating factor (GM-CSF) (1.7-fold), but not TNF-α concentrations in bronchoalveolar fluids of *Hsf1*$^{-/-}$ mice, compared with those of WT animals, indicating that HSF1 behaved as a repressor of specific cytokine production in our model. To further investigate the mechanism of GM-CSF repression, we analyzed the NF-κB activity and IκB stability. The DNA binding NF-κB activity, in particular p50 homodimer activity, was higher in *Hsf1*$^{-/-}$ mice than in wild-type mice after cadmium exposure. These results provide a first line of evidence that mechanisms of lung protection depending on HSF1 involve specific cytokine repression via inhibition of NF-κB activation, *in vivo*.

Keywords : Knockout Mice; Cadmium; Heat-Shock Proteins; Granulocyte-Macrophage Colony-Stimulating Factor.

Introduction

Heat shock transcription factor 1 (HSF1) is a major regulator of the heat shock (HS) response, a ubiquitous and phylogenetically conserved mechanism of cellular defense (36). This response is well known to involve the synthesis of heat shock proteins (Hsps), in cells that encounter various proteotoxic conditions, including heat shock, heavy metal exposure, alterations in the intracellular redox environment, and pathogen infection (12, 33). The clinical importance of this regulatory pathway is clearly demonstrated by a significant improvement of cell survival or organ function, including respiratory system, correlated with the overexpression of Hsps, after a variety of stresses such as sepsis, ischemia-reperfusion, and cytotoxic agent exposure (11, 34, 44).

However, HS response-mediated protection might involve mechanisms other than Hsp induction. Many data indicated that activation of HS response could inhibit the production of cytokines in response to pro-inflammatory stimulation (9, 25, 27, 28). Furthermore, the increased level of TNF-α recorded in HSF1-deficient mice, in parallel with their higher susceptibility to endotoxin challenge compared with wild-type animals, suggested a link between HSF1 and inhibition of this cytokine expression (45). HSF1 could act as a transcriptional repressor of pro-inflammatory genes as identified for TNF-α and interleukin 1β genes in endotoxin-stimulated macrophages (7, 38). Nevertheless, the mechanisms that govern the HS response-mediated inhibition of the pro-inflammatory processes, as well as the causal relationship between HSF1 and this inhibition remain to be investigated.

Since NF-κB is a major regulator of many pro-inflammatory genes, including TNF-α and granulocyte-macrophage colony-stimulating factor (GM-CSF) (4), an increasing interest has been

focused on HS preconditioning-induced inhibition of NF-κB activation in response to pro-inflammatory stimuli (30, 42, 47). Although HSF1 was suspected to be involved in this HS-mediated effect, recent data obtained with *Hsf1*$^{-/-}$ embryonic fibroblasts suggested that HSF1 was not responsible for this inhibition (29). Therefore, a better understanding of the role of HSF1 in NF-κB pathway inhibition requires further investigations in other cell types, and also in intact animals. This question was directly addressed in this work using Hsf1 knockout mice exposed to cadmium (Cd).

Cd provokes lung damage and inflammation (1, 3, 31), involving cytokine production (24). Interestingly, this heavy metal is also known as a strong inducer of the HS response (15, 40). The protective role of HSF1 against Cd-induced lung injuries has been recently identified (41) but the possible interactions between HSF1 and pro-inflammatory pathways were not known. *In vitro* studies showed that Cd activated the HSF1 and NF-kB pathways by increasing the level of oxidative stress (8, 14, 20, 21), but both phenomena were analysed separately.

The objective of this study was to examine *in vivo* whether the HSF1-mediated protection induced by Cd against its own toxic effects involved an inhibition of TNF-α and GM-CSF, two cytokines thought to play a part in Cd-induced inflammation in the lung. Furthermore, a potential interaction between HSF1 and NF-κB was investigated by measuring the level of activation of this factor in wild-type and HSF1-deficient mice after intranasal instillation of Cd.

Materials and Methods

Mice

Experiments were performed in wild-type (WT) and HSF1-deficient (*Hsf1*$^{-/-}$) female mice (body weight =20 ± 1 g, about 9-weeks old). Wild-type C57BL/6 mice were purchased from Charles River Laboratoties (IFFA CREDO, Bruxelles, Belgium). *Hsf1*$^{-/-}$ mice were obtained from the laboratory of Ivor Benjamin (UTSouthwestern Medical Center, Texas) and have been previously described (45). A breeding colony of *Hsf1*$^{-/-}$ knockout mice with an enriched C57BL/6 background was developed in our animal facility (FVM, University of Liege, Belgium) by mating *Hsf1*$^{+/-}$ males with wild-type C57BL/6 females for 5 or 6 generations. Then, *Hsf1*$^{+/-}$ males and females were intercrossed to produced *Hsf1*$^{-/-}$ mice with > 99 % of C57BL/6 background. Mice were housed in a temperature- and humidity-controlled animal house, maintained at 21°C with a 12-hours light-dark cycle. A balanced diet and water were supplied *ad libitum*. The ethics committee of the University of Liege approved the study.

Cadmium treatments

Cd was administered by intranasal instillation to WT or *Hsf1*$^{-/-}$ mice following anesthesia by intraperitoneal (ip) injection of a mixture of medetomidine (Orion, Finland) and ketamine (Merial, France) (0.6 µg/g and 0.04 mg/g body weight, respectively). For intranasal instillation, a Gilson pipette was used to dispense 20 µl of saline solution containing 0 (control), 10 or 100 µg of $CdCl_2$ in the nasal cavities.

Bronchoalveolar lavage (BAL) procedure and analyses

Mice were sacrificed by cervical dislocation immediately after plethysmography. Lungs were washed with 1 ml of PBS (Gibco, Paisley, UK), through a tracheal cannula and about 0.7 ml BAL was collected. BAL was centrifuged (5000*g* for 2 minutes), and the supernatant fluid phase was aliquoted and stored at -80 °C until cytokine and protein concentrations were assessed. Pelleted cells were resuspended in 200 µl of PBS. Total cells were counted with a hemocytometer and cell differentials determined in 200 µl of BAL fluid on Cytospin slides stained with May-Grunwald and Giemsa stain (Merck, Darmstradt, Germany). The protein concentration in cell-free BAL was determined by Bicinchoninic acid protein assay (Pierce, Perbioscience, Erembodegem, Belgium) with bovine serum albumin as a standard.

Cytokine assays

The concentrations of TNF-α and GM-CSF were quantified in the BAL fluid supernatants by enzyme-linked immunosorbent assay (ELISA) using mouse-specific kits (BioSource International, Nivelles, Belgium), according to the manufacturer's instructions. In each reaction well, 100 µl of sample was added to reagents without dilution.

Nuclear and cytoplasmic proteins extraction, Electrophoretic mobility shift assays (EMSAs), and Western blot analysis

Nuclear proteins were extracted from left washed lungs as previously described (6). Briefly, sample was homogenized in 5 ml of cytoplasmic buffer, containing 10 mM Hepes, pH 7.9, 10 mM KCl, 2 mM $MgCl_2$, 0.1 mM ethylenediaminetetraacetic acid (EDTA), 0.2% Nonidet P-40, and 1.6 mg/ml protease inhibitors (Complete; Boehringer Mannheim, Mannheim, Germany), and

supplemented with 3 mM of the protease inhibitor diisopropyl fluorophosphate (Sigma, Bornem, Belgium). Extracts were centrifuged (1500g, 5 minutes at 4°C). Pelleted nuclei were washed and resuspended in nuclear buffer (20 mM Hepes, pH 7.9, 1.5 mM $MgCl_2$, 0.2 mM EDTA 0.63 M NaCl, 25% glycerol, 1.6 mg/ml protease inhibitors, 3 mM diisopropyl fluorophosphates), incubated for 20 minutes at 4°C and centrifuged for 15 minutes at 11000 g. Protein was quantified in supernatants with the Micro BCA protein assay reagent kit (Pierce, Rockford, IL). A ^{32}P-labeled oligonucleotide containing the consensual κB sequence (6) or the consensual HSE sequence (5'-CTAGAAGCTTCTAGAAGCTTCTAG-3') was used as the probe in EMSAs. The amount of specific complexes was determined by photodensitometry of the autoradiography. Supershift experiments were also performed as previously described (6), using rabbit antibodies recognizing the specific NF-κB subunits p50, p52, p65, RelB, and c-Rel. The antibodies were purchased from Santa Cruz Biotechnology Inc. (Santa Cruz, CA, USA).

Cytoplasmic protein extracts (10 µg) were added to a loading buffer (10 mM Tris-HCl (pH 6.8), 1% (w/v) SDS, 25% (v/v) glycerol, 0.1 mM 2-ME, and 0.03% (w/v) bromophenol blue), boiled, and run on a 10% SDS-PAGE gel. After electrotransfer to polyvinylidene difluoride membranes (Roche, Mannheim, Germany) and blocking overnight at 4°C with 20 mM Tris (pH 7.5), 500 mM NaCl, 0.2 (v/v) Tween 20 (Tris-HCl/Tween), and 5% (w/v) dry milk, the membranes were incubated for 1 hour with a rabbit polyclonal recognizing mouse IκB-α (1/1000 dilution), washed and then incubated for 45 minutes with peroxidase-conjugated goat anti-rabbit IgG (1/2000 dilution) (Kirkegaard & Perry, Gaithersburg, MD). The results of the reaction were revealed with the enhanced chemiluminescence detection method (ECL kit; Amersham Pharmacia Biotech, Aylesbury, U.K.).

Lung histology

The washed lungs were dissected and infused with 4% buffered formaldehyde at 25 cm H_2O pressure via a tracheal cannula until all pulmonary lobes were fully inflated. After overnight fixation in the same fixative at 4°C, the lung tissue was embedded in paraffin using conventional methods. Five micron tissue sections were stained with hematoxylin-eosin. Degree of microscopic lung injury was analyzed using a semiquantitative system. Three sites on each slide were evaluated for several variables (congestion, septal thickening, edema, hemorrhage, and neutrophils infiltration) and given relative scores. For each component, the extent of injury was assigned a score of 0 (no injury), 1 (injury to 25% of the field), 2 (25-50%) or 3 (more than 50%), and the severity was graded as 0, 1, 2, or 3. A mean score for each variable for each animal was expressed as the sum of extent and severity.

Lung wet-to-dry weight ratio

The wet weight of whole lungs was measured on an electronic scale immediately after euthanasia. The lungs were then desiccated in an oven at 65°C for 72 hours to determine the dry weight.

Statistical analysis

Data are expressed as the mean ± standard deviation and were analyzed using Statistica for Windows software (StatSoft Inc., Tulsa, OK, USA). Data were normally distributed (Levene median test). The effects of Cd dose, genotype and time after instillation were assessed by analysis of variance (ANOVA) with three factors. Statistical comparisons between and within groups were made by post-hoc Tukey's test. Levels of significance were set at $p < 0.05$.

Results

Cd-induced lung injury in WT and Hsf1$^{-/-}$ mice

To define the HSF1-mediated protection in Cd-induced lung injury, WT and *Hsf1*$^{-/-}$ mice were exposed to 10 or 100 µg Cd by intranasal instillation. Number of total cells, macrophages and neutrophils, as well as protein concentration in BAL fluids, lung wet-to-dry weight ratio and histopathology were evaluated 4, 10 and 24 hours after the Cd instillation as indices of the pathophysiological response. No changes were recorded up to 24 hours following saline instillation, and there were no significant differences between the values recorded in WT and *Hsf1*$^{-/-}$ control mice (Figs. 1, 2 and 3). Cells in BAL fluids counted in control mice and before instillation were predominantly macrophages.

Compared with saline administration, both Cd doses caused progressive increase in the number of total cells, macrophages and neutrophils in BAL fluids sampled from WT mice (Fig. 1). The first significant change in the total cell count was observed 24 hours after instillation of 10 µg and 10 hours after 100 µg Cd. The changes occurring in mice exposed to the low and high Cd doses were partly due to an increase in the macrophage number (4.2- and 10.6-fold) but mainly explained by a marked rise in the neutrophil count (53- and 62-fold, respectively). In *Hsf1*$^{-/-}$ animals, Cd provoked also a time- and dose-dependent increase in cell counts, compared with their respective controls. However, in comparison with WT mice, the total cell, macrophage and neutrophil numbers were significantly higher in these mice 24 hours after the two Cd doses.

Lung wet-to-dry weigh ratio and BAL fluid protein were significantly increased by Cd instillation in WT mice (Fig 2). Lung wet-to-dry weigh ratio reached high levels 10 hours after 10 µg and 4

hours after 100 µg, indicating significant edema, congestion and/or hemorrhage. Proteins in BAL fluids reached maximal concentrations 10 hours after 10 µg and 100 µg, confirming lung edema. The responses recorded in Cd-exposed *Hsf1*$^{-/-}$ mice followed the same kinetics, but the magnitude of the maximal changes was higher in these mice than in WT mice.

Tissue congestion and hemorrhage were observed macroscopically in some portions of the Cd-treated lungs, in comparison with controls. Figure 3 shows light photographs of representative lung tissue from WT (A, C and E) and *Hsf1*$^{-/-}$ mice (B, D and F) exposed to either saline or Cd (10 µg or 100 µg). In saline-treated WT and *Hsf1*$^{-/-}$ mice, lungs appeared normal, with intact parenchyma and without inflammatory injury (Figs. 3A and B). 24 hours after 10 µg Cd instillation, the WT mice exhibited marked pathological changes in the peribronchiolar regions and throughout the alveoli (Figs. 3C vs A). Inflammation was evident and characterized by neutrophil and macrophage infiltration into interalveolar septa and peribronchiolar tissues, as well as interstitium thickening and congestion. Some alveoli seemed also filled with sloughed material perhaps due to edema and cytolysis. This lung damage was most severe after the high dose of Cd (Fig. 3E vs C), and was significantly more prominent in *Hsf1*$^{-/-}$ mice (Figs. 3D and F vs C and E), as shown by histological quantification.

TNF-α, GM-CSF expression in WT and Hsf1*$^{-/-}$ *mice after Cd exposure

To examine whether the HSF1-mediated protection described above in WT mice, when compared with *Hsf1*$^{-/-}$ mice, was associated with an alteration of cytokine expression, TNF-α and GM-CSF concentrations were determined in BAL fluids from WT and *Hsf1*$^{-/-}$ mice 4, 10, and 24 hours after Cd instillation. The BAL fluids of mice constitutively contained both TNF-α and GM-CSF,

and there were no changes up to 24 hours following saline treatment. No differences were detected between TNF-α and GM-CSF concentrations in WT and *Hsf1*$^{-/-}$ control mice (Fig. 4).

Cd increased the TNF-α concentration, in a dose-dependent manner, in the BAL fluids of WT animals (Fig. 4A). Maximal increase in TNF-α was recorded 24 hours after both 10 and 100 µg of Cd, as described above regarding the inflammatory cell influx in BAL fluids. The TNF-α concentrations in BAL fluids were not significantly different between WT and *Hsf1*$^{-/-}$ mice, whatever the Cd dose.

In contrast, instillation of Cd was followed by a peak of GM-CSF concentration 10 hours after both 10 and 100 µg, indicating that GM-CSF release preceded macrophage and neutrophil recruitment. In addition, the GM-CSF concentrations were significantly higher in *Hsf1*$^{-/-}$ animals compared to WT mice.

NF-κB activation and I-κB degradation in WT and Hsf1*$^{-/-}$ *mice after Cd exposure

As GM-CSF expression is modulated by HSF1 and as NF-κB is a major regulator of pro-inflammatory processes (4), the effect of HSF1 on NF-κB activation was investigated by measuring the NF-κB DNA-binding activity in the lungs of WT and *Hsf1*$^{-/-}$ mice 4 and 24 hours after Cd instillation.

The lungs of saline-treated WT mice exhibited weak basal NF-κB binding activity (Fig. 5A). Cd induced marked NF-κB activation as early as 4 hours after instillation of both doses in these mice, indicating that NF-κB activation in lung tissue preceded cytokine release in BAL fluids. In

addition, binding activity level remained elevated at 24 hours. While the basal NF-κB binding activity was not different in the WT and *Hsf1*$^{-/-}$ mice, the level of activity was significantly higher in the latter animals than in the former, 4 and 24 hours after Cd instillation, as shown by densitometry. Nuclear extracts from all Cd-treated mice exhibited activation of distinct NF-κB complexes as shown by the two bands detected in each sample. While the lower band was systematically more intense in *Hsf1*$^{-/-}$ than in WT mice, this difference was clearly less marked for the upper bands.

To characterize the NF-κB complexes, supershift experiments using antibodies directed against the various members of the NF-κB family (i.e., p50, p52, p65, RelB, and cREL) were performed (Fig. 5B). Anti-p50 antibodies supershifted the faster migrating complex (lower band) and partially the slower migrating complex (upper band), which was also supershifted by anti-p65 antibodies. This identified the two specific Cd-activated NF-κB complexes as the p50 homodimer and the p65/p50 heterodimer. These results, together with the analysis of NF-κB activity, suggested that the binding activity of p65/p50 heterodimer, and particularly of p50 homodimer, was higher in HSF1-deficient mice compared with WT mice (Fig 5A and B).

Having demonstrated that HSF1 inhibited Cd-mediated NF-κB activation, we therefore wanted to determine the effect of HSF1 on I-κB stability after Cd instillation. Treatment with 10 and 100 µg of Cd caused rapid degradation of I-κB in both the WT and *Hsf1*$^{-/-}$ mice compared to controls (Fig 5C). The Cd-induced I-κB degradation was more marked in *Hsf1*$^{-/-}$ animals compared to WT mice, 24 hours after instillation.

HSF1 activation in WT mice after Cd exposure

Results based on use of $HSF1^{-/-}$ mice indicated a role of HSF1 in lung protection against Cd, involving inhibition of pro-inflammatory processes. To attribute and confirm the functional role for HSF1 in our model, activation of this factor by cadmium and kinetics of its activation was investigated by measuring the HSF1 binding activity in the lungs of WT mice 1, 2, 3, 4, 10 and 24 hours after Cd instillation. As shown in Figure 6, Cd increased DNA-binding activity of HSF1 relative to that seen in corresponding control animals. This increase reached maximal magnitude 2 hours after Cd exposure and after that the induction disappeared. Therefore, HSF1 activation preceded NF-κB inhibition.

Discussion

The inhibition of inflammatory response to various insults by the HS response involves different pathways protecting cells, organs, or organisms. Although the involved mechanisms are not yet clearly elucidated, Hsps and their major regulatory partner HSF1 are recognized as playing an important role in this protection. However, while prior induction of HS response could modulate the activation of NF-κB and the production of cytokines in response to a pro-inflammatory stimuli (42, 43, 47), the involvement of HSF1 in this effect has remained a matter of debate (29, 45). Using HSF1-deficient mice enabled us to unambiguously identify the role of this factor in the HS response effects on the lung damage, NF-κB activation and cytokine release, after Cd exposure.

Our results confirmed that acute Cd exposure elicited HSF1-dependent protective mechanisms against its own toxic effects, as recently characterized in mice (41). Indeed, compared with WT mice, *Hsf1*$^{-/-}$ mice exhibited higher lung wet-to-dry weight ratios after intranasal instillation of 10 µg Cd and more marked increase in protein concentrations and inflammatory cell numbers in BAL fluids confirming the more severe histopathological signs of lung damage detected after 10 and 100 µg. The investigation of the cytokine concentrations in BAL fluids indicated that Cd stimulated both TNF-α and GM-CSF pulmonary expression in mice. The increase in the TNF-α concentration in BAL fluids, occurring simultaneously with the increase in macrophage and neutrophil numbers, might be interpreted as a consequence rather than a mediator of the inflammatory cell influx. This was in accordance with previous data showing that TNF-α was not responsible for the hepathotoxicity in mice exposed to Cd (79). In contrast, GM-CSF increase, preceding maximal macrophage and neutrophil influx, could play an important role in the

inflammatory cell recruitment in our model. GM-CSF promotes the growth of myeloid progenitor cells and can regulate the accumulation, the survival and the activity of macrophages and neutrophils (2). The principal source of GM-CSF is activated epithelial cells and macrophages (35, 46), two cell types affected by Cd in the lung (5, 19, 31). In addition, only GM-CSF concentrations were higher in *Hsf1*$^{-/-}$ than in WT mice indicating that HSF1-mediated lung protection was related to an inhibition of GM-CSF expression. This confirms that HSF1 was a repressor of cytokine expression, in agreement with Xiao *et al*. (45). As all these changes occurred after the increase in lung wet-to-dry weight ratio and BAL fluid protein, one can assume that the pathophysiological mechanisms leading to edema, in our model, were not directly dependent on TNF-α and GM-CSF.

As previously described in cultured cells (8, 20), exposure to Cd activated NF-κB in lungs. The inhibition of NF-κB activation was strongly suspected to play a role in the mechanisms of the HSF1-mediated inhibition of the pro-inflammatory response (30), but the causal relationship between HSF1 and this inhibition remained to be determined. In the present study, the level of NF-κB binding activity in *Hsf1*$^{-/-}$ mice after 10 and 100 µg Cd was clearly higher than that in WT mice.. This is the first *in vivo* evidence of an effect of HSF1 on NF-κB. In addition, HSF1 activity was clearly enhanced by Cd, this activation preceded NF-κB inhibition, confirming functional and temporal role of HSF1 in inhibition of this pro-inflammatory pathway. The exact mechanism by which the HSF1 pathway affected NF-κB activation has not been determined in this work. The findings of Feinstein *et al.* (13), which showed that overexpression of Hsp70, induced by HS preconditioning or transfection of *hsp70* gene in astroglial cells, inhibited the NF-κB activation argued in favour of the central role played by Hsps (13). However, a modulating effect of Hsp70 on NF-κB activation in mice exposed to intranasal Cd instillation is unlikely, at least during the

early toxic effects, since the pulmonary Hsp70 expression was not yet detected at 4 hours following the Cd administration (41) while HSF1-mediated inhibition of NF-κB activation was already marked at this moment in the current study. Besides, it was demonstrated in cultured respiratory epithelial cells preconditioned by HS or sodium arsenite, that stabilization of the NF-κB inhibitory protein, IκB, by the HS response is involved in the inhibition of cytokine-mediated NF-κB activation (43, 47). In accordance with this observation, the Cd-induced degradation of IκB-α was inhibited by HSF1 pathway in our *in vivo* model, but only 24 hours after treatment. Hsps might be involved at this level. The HS-induced prevention of IκB kinase (IKK) activation leading to the inhibition of the IκB phosphorilation is an alternative pathway susceptible to modulate the NF-κB activity (10, 26, 47), but evidence for the role of HSF1 in this effect is still lacking. Finally, GM-CSF can regulate NF-κB activity. HSF1-mediated inhibition of GM-CSF expression could then reinforce inhibition of NF-κB activation. Taken together, our results suggest that, during the early Cd-induced lung injuries, an interaction between HSF1 and NF-κB seems to be involved in the protective effect of the heat shock response. Afterward, at 24 hours after Cd instillation, different mechanisms could contribute to inhibition of NF-κB pathway, but HSF1 appears still as a major mediator of these ones.

As mentioned above, the comparison of cytokine production in WT and *Hsf1*$^{-/-}$ mice, revealed that HSF1 moderated GM-CSF expression in response to Cd. In contrast, the lack of influence of HSF1 on TNF-α raises a question about the role played by NF-κB in the control of these cytokines since its activity was higher in *Hsf1*$^{-/-}$ mice. A possible explanation could be given by the differential effect of p65/p50 heterodimer and p50 homodimer on cytokine expression, according to their respective activity. While the levels of binding activity of both complexes were

higher in *Hsf1*$^{-/-}$ mice compared to WT animals, the difference was especially marked regarding p50. This complex is suspected to have a specific repressor effect on the TNF-α gene but not on GM-CSF gene (22), while p65/p50 is activator of both cytokines expression (4, 17). Therefore, the Cd-induced TNF-α expression depends on the combination of opposite actions of both p65/p50 and p50. In *Hsf1*$^{-/-}$ mice, the repressive effect of the high level of p50 activity could abrogate the positive effect of p65/p50 on TNF-α. In contrast, the control of GM-CSF is less complex, and the higher GM-CSF concentrations recorded in *Hsf1*$^{-/-}$ mice could result from the positive control exerted by p65/p50, while p50 did not influence this control. A verification of this hypothesis will require further experiments.

In summary, several pathways appear to contribute to HS response-mediated lung protection against chemical-induced lung injury, including cytoprotective functions of Hsps under the control of HSF1 and interaction between the HS response and pro-inflammatory process (30, 44). In Cd-induced lung injury model, the inhibition of inflammatory responses by the HS response involves a decrease of cytokine expression, particularly of GM-CSF, which was related to an inhibition of NF-kB activation. This is the first *in vivo* demonstration that HSF1 is a major mediator of this latter effect. Given the fundamental roles of the HS response and the NF-κB pathway in cellular function, it is probable that the interaction between HSF1 and NF-κB has the potential to impact on the course and outcomes of critically ill patients.

Acknowledgements

This work was supported by grant agencies: FNRS-FRIA and FRSM. We acknowledge the dedicated work of M. Belleflamme who performed all cell counts in BAL fluids. We thank also E.M. McNamara and L. Fievez.

References

1. **Bajpai R, Waseem M, Khanna AK and Kaw JL**. Comparative pulmonary toxicity of cadmium and nickel: histopathological and bronchoalveolar lavage analysis. *Indian J Exp Biol* 37: 541-545, 1999.

2. **Baldwin GC**. The biology of granulocyte-macrophage colony-stimulating factor: effects on hematopoietic and nonhematopoietic cells. *Dev Biol* 151: 352-367, 1992.

3. **Bell RR, Nonavinakere VK and Soliman MR**. Intratracheal exposure of the guinea pig lung to cadmium and/or selenium: a histological evaluation. *Toxicol Lett* 114: 101-109, 2000.

4. **Blackwell TS and Christman JW**. The role of nuclear factor-kappa B in cytokine gene regulation. *Am J Respir Cell Mol Biol* 17: 3-9, 1997.

5. **Buckley BJ and Bassett DJ**. Pulmonary cadmium oxide toxicity in the rat. *J Toxicol Environ Health* 21: 233-250, 1987.

6. **Bureau F, Bonizzi G, Kirschvink N, Delhalle S, Desmecht D, Merville MP, Bours V and Lekeux P**. Correlation between nuclear factor-kappaB activity in bronchial brushing samples and lung dysfunction in an animal model of asthma. *Am J Respir Crit Care Med* 161: 1314-1321, 2000.

7. **Cahill CM, Waterman WR, Xie Y, Auron PE and Calderwood SK**. Transcriptional repression of the prointerleukin 1beta gene by heat shock factor 1. *J Biol Chem* 271: 24874-24879, 1996.

8. **Camhi SL, Lee P and Choi AM**. The oxidative stress response. *New Horiz* 3: 170-182, 1995.

9. **Chu EK, Ribeiro SP and Slutsky AS**. Heat stress increases survival rates in lipopolysaccharide-stimulated rats. *Crit Care Med* 25: 1727-1732, 1997.

10. **Curry HA, Clemens RA, Shah S, Bradbury CM, Botero A, Goswami P and Gius D**. Heat shock inhibits radiation-induced activation of NF-kappaB via inhibition of I-kappaB kinase. *J Biol Chem* 274: 23061-23067, 1999.

11. **De Maio A**. Heat shock proteins: facts, thoughts, and dreams. *Shock* 11: 1-12, 1999.

12. **Feige U, Morimoto RI, Yahara I and Polla BS**. Stress-inducible cellular responses. Basel-Boston-Berlin: Birkhäuser-Verlag, 1996.

13. **Feinstein DL, Galea E, Aquino DA, Li GC, Xu H and Reis DJ**. Heat shock protein 70 suppresses astroglial-inducible nitric-oxide synthase expression by decreasing NFkappaB activation. *J Biol Chem* 271: 17724-17732, 1996.

14. **Galan A, Troyano A, Vilaboa NE, Fernandez C, de Blas E and Aller P**. Modulation of the stress response during apoptosis and necrosis induction in cadmium-treated U-937 human promonocytic cells. *Biochim Biophys Acta* 1538: 38-46, 2001.

15. **Gaubin Y, Vaissade F, Croute F, Beau B, Soleilhavoup J and Murat J**. Implication of free radicals and glutathione in the mechanism of cadmium-induced expression of stress proteins in the A549 human lung cell-line. *Biochim Biophys Acta* 1495: 4-13, 2000.

16. **Georgopoulos C and Welch WJ**. Role of the major heat shock proteins as molecular chaperones. *Annu Rev Cell Biol* 9: 601-634, 1993.

17. **Ghosh S, May MJ and Kopp EB**. NF-kappa B and Rel proteins: evolutionarily conserved mediators of immune responses. *Annu Rev Immunol* 16: 225-260, 1998.

18. **Hamelmann E, Schwarze J, Takeda K, Oshiba A, Larsen GL, Irvin CG and Gelfand EW**. Noninvasive measurement of airway responsiveness in allergic mice using barometric plethysmography. *Am J Respir Crit Care Med* 156: 766-775, 1997.

19. **Hart BA, Gong Q, Eneman JD and Durieux-Lu CC**. In vivo expression of metallothionein in rat alveolar macrophages and type II epithelial cells following repeated cadmium aerosol exposures. *Toxicol Appl Pharmacol* 133: 82-90, 1995.

20. **Hart BA, Lee CH, Shukla GS, Shukla A, Osier M, Eneman JD and Chiu JF**. Characterization of cadmium-induced apoptosis in rat lung epithelial cells: evidence for the participation of oxidant stress. *Toxicology* 133: 43-58, 1999.

21. **Hung JJ, Cheng TJ, Lai YK and Chang MD**. Differential activation of p38 mitogen-activated protein kinase and extracellular signal-regulated protein kinases confers cadmium-induced HSP70 expression in 9L rat brain tumor cells. *J Biol Chem* 273: 31924-31931, 1998.

22. **Ishikawa H, Claudio E, Dambach D, Raventos-Suarez C, Ryan C and Bravo R**. Chronic inflammation and susceptibility to bacterial infections in mice lacking the polypeptide (p)105 precursor (NF-kappaB1) but expressing p50. *J Exp Med* 187: 985-996, 1998.

23. **Jang AS, Choi IS, Koh YI, Park CS and Lee JS**. The relationship between alveolar epithelial proliferation and airway obstruction after ozone exposure. *Allergy* 57: 737-740, 2002.

24. **Kataranovski M, Kataranovski D, Savic D, Jovcic G, Bogdanovic Z and Jovanovic T**. Granulocyte and plasma cytokine activity in acute cadmium intoxication in rats. *Physiol Res* 47: 453-461, 1998.

25. **Klosterhalfen B, Hauptmann S, Offner FA, Amo-Takyi B, Tons C, Winkeltau G, Affify M, Kupper W, Kirkpatrick CJ and Mittermayer C**. Induction of heat shock

protein 70 by zinc-bis-(DL-hydrogenaspartate) reduces cytokine liberation, apoptosis, and mortality rate in a rat model of LD100 endotoxemia. *Shock* 7: 254-262, 1997.

26. **Kohn G, Wong HR, Bshesh K, Zhao B, Vasi N, Denenberg A, Morris C, Stark J and Shanley TP**. Heat shock inhibits tnf-induced ICAM-1 expression in human endothelial cells via I kappa kinase inhibition. *Shock* 17: 91-97, 2002.

27. **Lappas GD, Karl IE and Hotchkiss RS**. Effect of ethanol and sodium arsenite on HSP-72 formation and on survival in a murine endotoxin model. *Shock* 2: 34-39, 1994.

28. **LoCicero J, III, Xu X and Zhang L**. Heat shock protein suppresses the senescent lung cytokine response to acute endotoxemia. *Ann Thorac Surg* 68: 1150-1153, 1999.

29. **Malhotra V, Eaves-Pyles T, Odoms K, Quaid G, Shanley TP and Wong HR**. Heat shock inhibits activation of NF-kappaB in the absence of heat shock factor-1. *Biochem Biophys Res Commun* 291: 453-457, 2002.

30. **Malhotra V and Wong HR**. Interactions between the heat shock response and the nuclear factor- kappaB signaling pathway. *Crit Care Med* 30: S89-S95, 2002.

31. **McKenna IM, Waalkes MP, Chen LC and Gordon T**. Comparison of inflammatory lung responses in Wistar rats and C57 and DBA mice following acute exposure to cadmium oxide fumes. *Toxicol Appl Pharmacol* 146: 196-206, 1997.

32. **McMillan DR, Xiao X, Shao L, Graves K and Benjamin IJ**. Targeted disruption of heat shock transcription factor 1 abolishes thermotolerance and protection against heat-inducible apoptosis. *J Biol Chem* 273: 7523-7528, 1998.

33. **Morimoto RI, Kline MP, Bimston DN and Cotto JJ**. The heat-shock response: regulation and function of heat-shock proteins and molecular chaperones. *Essays Biochem* 32: 17-29, 1997.

34. **Morimoto RI and Santoro MG**. Stress-inducible responses and heat shock proteins: new pharmacologic targets for cytoprotection. *Nat Biotechnol* 16: 833-838, 1998.

35. **Nimer SD and Uchida H**. Regulation of granulocyte-macrophage colony-stimulating factor and interleukin 3 expression. *Stem Cells* 13: 324-335, 1995.

36. **Santoro MG**. Heat shock factors and the control of the stress response. *Biochem Pharmacol* 59: 55-63, 2000.

37. **Sciuto AM, Lee RB, Forster JS, Cascio MB, Clapp DL and Moran TS**. Temporal changes in respiratory dynamics in mice exposed to phosgene. *Inhal Toxicol* 14: 487-501, 2002.

38. **Singh IS, He JR, Calderwood S and Hasday JD**. A high affinity HSF-1 binding site in the 5'-untranslated region of the murine tumor necrosis factor-alpha gene is a transcriptional repressor. *J Biol Chem* 277: 4981-4988, 2002.

39. **Vincke G, Denhaive P, Striernet F, Peck M and Gustin P**. Pulmonary inflammatory response of rats exposed to repeated nebulizations of cadmium. *Am J Respir Crit Care Med* 165: A48, 2002.

40. **Wirth D, Christians ES, Munaut C, Dessy C, Foidart J-M and Gustin P**. Differential heat shock gene *hsp70-1* response to toxicants revealed by in vivo study of lungs in transgenic mice. *Cell Stress Chaperones* 7: 387-395, 2002.

41. **Wirth D, Christians ES, Li X, Benjamin IJ and Gustin P**. Use of *Hsf1*$^{-/-}$ mice reveals an essential role for HSF1 to protect lung against Cadmium-induced injury. *Toxicol Appl Pharmacol* 192: 12-20, 2003.

42. **Wong HR, Ryan M and Wispe JR**. Stress response decreases NF-kappaB nuclear translocation and increases I-kappaBalpha expression in A549 cells. *J Clin Invest* 99: 2423-2428, 1997.

43. **Wong HR, Ryan M and Wispe JR**. The heat shock response inhibits inducible nitric oxide synthase gene expression by blocking I kappa-B degradation and NF-kappa B nuclear translocation. *Biochem Biophys Res Commun* 231: 257-263, 1997.

44. **Wong HR and Wispe JR**. The stress response and the lung. *Am J Physiol* 273: L1-L9, 1997.

45. **Xiao X, Zuo X, Davis AA, McMillan DR, Curry BB, Richardson JA and Benjamin IJ**. HSF1 is required for extra-embryonic development, postnatal growth and protection during inflammatory responses in mice. *EMBO J* 18: 5943-5952, 1999.

46. **Xing Z, Braciak T, Ohkawara Y, Sallenave JM, Foley R, Sime PJ, Jordana M, Graham FL and Gauldie J**. Gene transfer for cytokine functional studies in the lung: the multifunctional role of GM-CSF in pulmonary inflammation. *J Leukoc Biol* 59: 481-488, 1996.

47. **Yoo CG, Lee S, Lee CT, Kim YW, Han SK and Shim YS**. Anti-inflammatory effect of heat shock protein induction is related to stabilization of I kappa B alpha through preventing I kappa B kinase activation in respiratory epithelial cells. *J Immunol* 164: 5416-5423, 2000.

48. **Zeldin DC, Wohlford-Lenane C, Chulada P, Bradbury JA, Scarborough PE, Roggli V, Langenbach R and Schwartz DA**. Airway inflammation and responsiveness in prostaglandin H synthase- deficient mice exposed to bacterial lipopolysaccharide. *Am J Respir Cell Mol Biol* 25: 457-465, 2001.

Figure legends

Figure 1. Total cell, macrophage and neutrophil counts in BAL fluids of WT and HSF1 deficient mice exposed to 10 µg (A) or 100 µg (B) Cd. Mice received an intranasal instillation of Cd or saline and were sacrificed for bronchoalveolar lavage 4, 10 or 24 hours after administration. Alveolar total cells, macrophages, and neutrophils were quantified. No significant changes were detected in other cell counts. Since no changes were recorded during 24 hours in saline-treated mice, all values were pooled and presented as controls values. Results are shown as mean ± SD (n = 5-6/time point). § $p<0.05$ for comparison with controls in the same group. * $p < 0.05$ for comparison with wild-type at the same time point. Significant difference was recorded between the two doses in the same type of animals ($p<0.05$, ANOVA).

Figure 2. Lung wet-to-dry weight ratios (A) and BAL fluid protein concentrations (B) in WT and Hsf1-deficient mice exposed to 10 µg or 100 µg Cd. Mice received an intranasal instillation of Cd or saline and were sacrificed 4, 10 or 24 hours after administration. Lungs were removed for determination of lung wet-to-dry weight ratio, or bronchoalveolar lavage was performed for protein evaluation. Since no changes were recorded during 24 hours in saline-treated mice, all values were pooled and presented as control values. Results are shown as mean ± SD (n = 5-6/time point). § $p<0.05$ for comparison with controls in the same group. * $p < 0.05$ for comparison with wild-type at the same time point. Significant difference was recorded between the two doses in the same type of animals ($p<0.05$, ANOVA).

Figure 3. Light micrographs of stained sections of washed lung from WT and HSF1 deficient mice 24 hours after intranasal instillation of Cd or saline. (A) Normal lung of WT mice; (B)

Normal lung of HSF1 deficient mice; (C) WT mice after instillation of 10 µg Cd showing generalized alveolar lesions (*gray arrow*), congestion (*blue arrowheads*), cell infiltration in interalveolar septa and interstitium (*black arrowheads*), and septa thickening; (D) HSF1 deficient mice after instillation of Cd 10 µg showing similar lesions to WT mice but more severe cell infiltration into peribronchiolar tissue (*black arrowhead*); (E) WT mice after instillation of Cd 100 µg showing oedema (*black arrow*) and cell infiltration; (F) HSF1 deficient mice after instillation of Cd 100 µg showing more severe alveolar lesions (*gray arrow*) and cell infiltration (*black arrowhead*). Magnification is x 250 for lung. Histogram shows degree of microscopic injury scored for each indicated variable. Histological results are presented as mean ± SD (n = 4/group). * $p < 0.05$ for comparison with wild-type mice after the same Cd dose. In all Cd-treated mice, significant difference with saline treated mice was recorded.

Figure 4. Release of TNF-α (A) and GM-CSF (B) in BAL fluids of WT and Hsf1-deficient mice exposed to 10 µg or 100 µg Cd. Mice received an intranasal instillation of Cd or saline and were sacrificed for bronchoalveolar lavage 4, 10 or 24 hours after administration. Cytokine concentrations in BAL fluids were determined by ELISA. Since no changes were recorded up to 24 hours in saline-treated mice, all values were pooled and presented as controls values. Results are shown as mean ± SD (n = 5-6/time point). § $p<0.05$ for comparison with controls in the same group. * $p < 0.05$ for comparison with wild-type at the same time point. Significant difference was recorded between the two doses in the same type of animals ($p<0.05$, ANOVA).

Figure 5. Representative analysis of NF-κB activation (A), specific active NF-κB complexes (B) and I-κB degradation (C) in the lungs of WT and Hsf1-deficient mice exposed to Cd. Mice

received an intranasal instillation of Cd or saline and were sacrificed 4 or 24h after administration. Nuclear and cytoplasmic extracts were prepared from lung tissue and analyzed for (A) NF-κB binding activity by EMSA and (C) IκB-α stability by Western blot, respectively. The line of mice, the dose of cadmium administered and the time at which animals were sacrificed are indicated above each lane. The *open* and *solid arrows* indicate specific slower and faster migrating NF-κB complexes. Histograms represent the mean (± SD) densitometry values of 4 individual experiments. § $p<0.05$ for comparison with controls in the same group. * $p < 0.05$ for comparison with wild-type at the same time point. (B) Characterization of specific active NF-κB complexes was performed by supershift analyses conduced with specific antibodies as indicated. The specific complexes are indicated by *arrows*. Supershifts of p50 and p65 are indicated by *closed and open arrowheads*, respectively. Ab, antodibodies.

Figure 6. Representative analysis of HSF1 activation in the lungs of WT mice exposed to Cd. Mice received an intranasal instillation of 100 µg Cd or saline and were sacrificed 1, 2, 3, 4, 10 or 24h after administration. Nuclear extracts were prepared from lung tissue and analyzed for HSF1 binding activity by EMSA. The time at which animals were sacrificed are indicated above each lane.

Figure 1

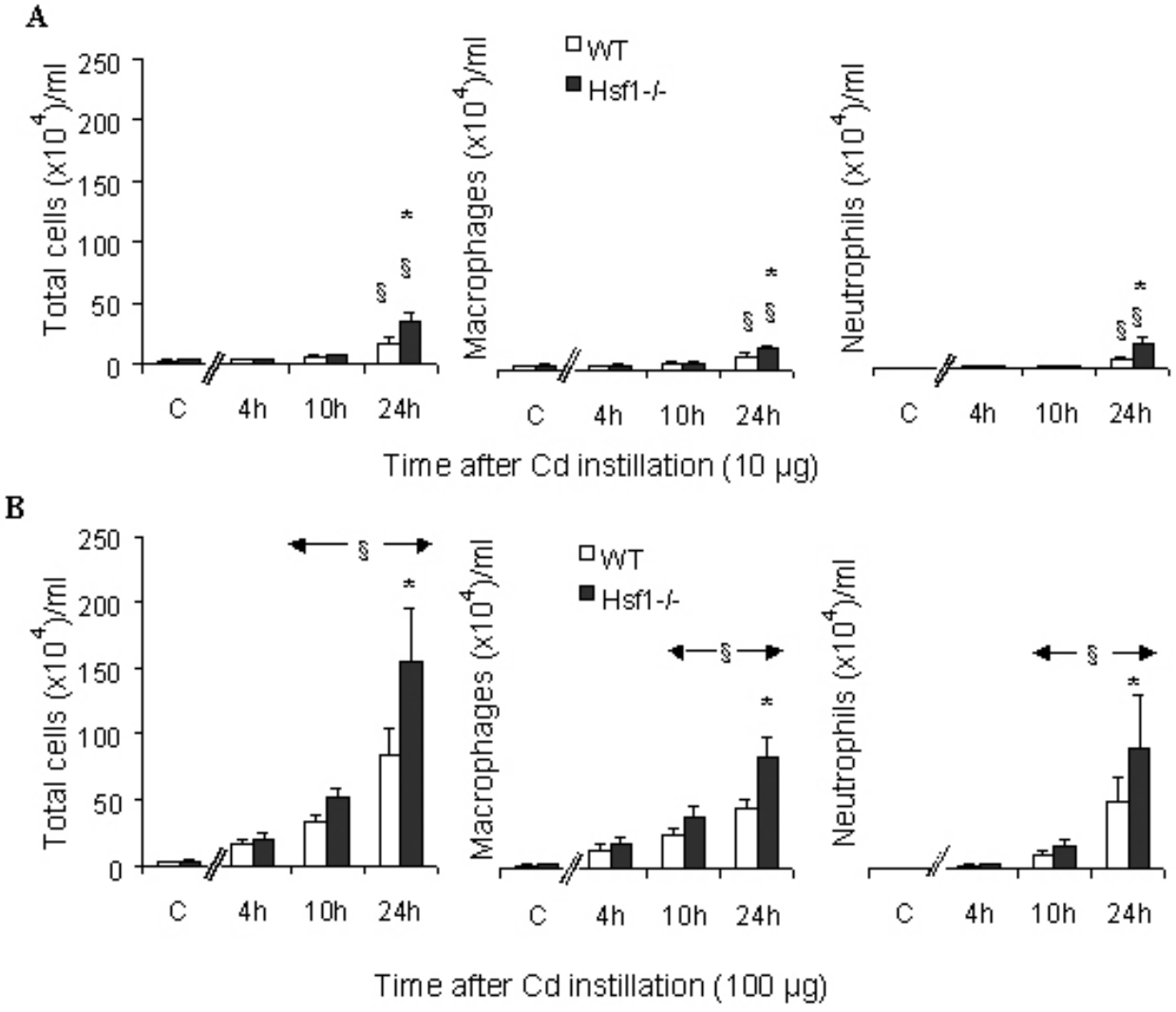
A
Total cells (x10^4)/ml
Macrophages (x10^4)/ml
Neutrophils (x10^4)/ml
WT
Hsf1-/-
0
50
100
150
200
250
C
4h
10h
24h
§
*
Time after Cd instillation (10 µg)
B
Time after Cd instillation (100 µg)

Figure 2

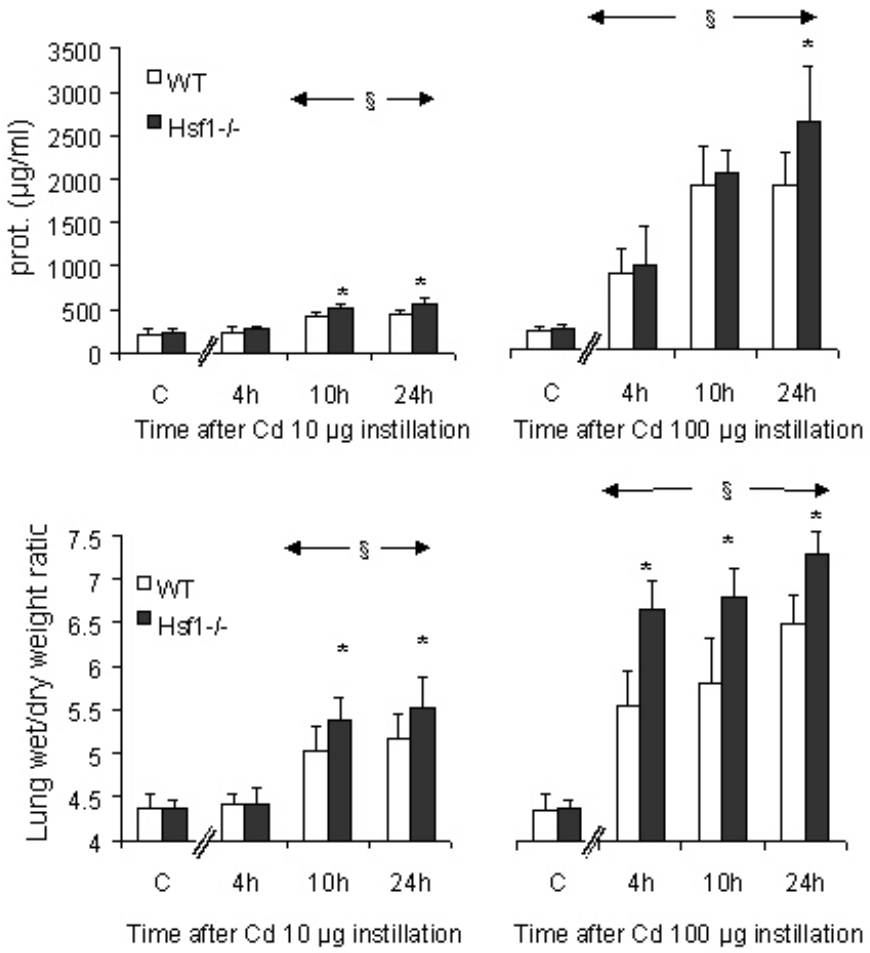
prot. (µg/ml)
3500
3000
2500
2000
1500
1000
500
0
WT
Hsf1-/-
§
*
C
4h
10h
24h
Time after Cd 10 µg instillation
Time after Cd 100 µg instillation
Lung wet/dry weight ratio
7.5
7
6.5
6
5.5
5
4.5
4

Figure 3

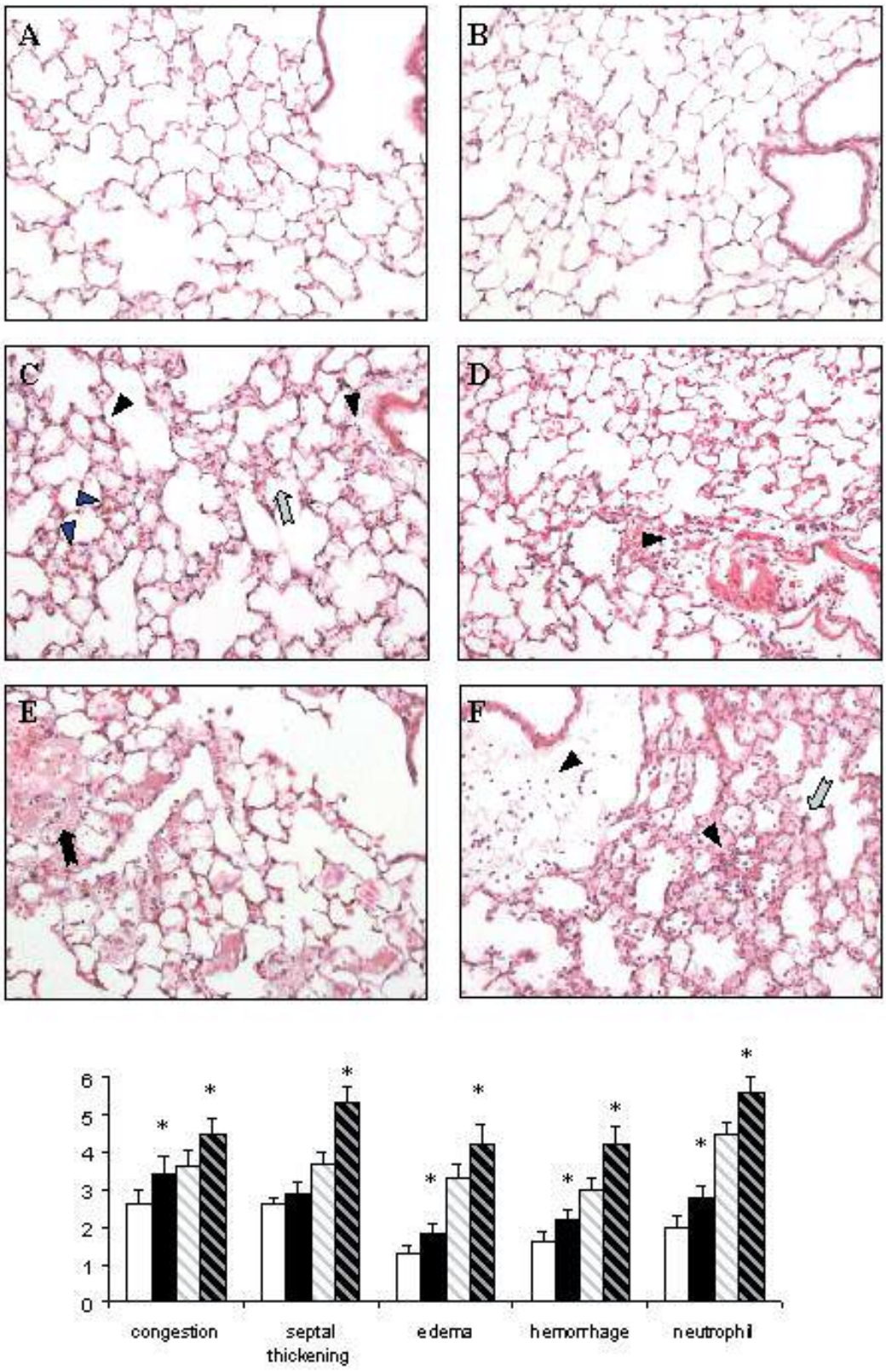
A
B
C
D
E
F
6
5
4
3
2
1
0
congestion
septal thickening
edema
hemorrhage
neutrophil

Figure 4

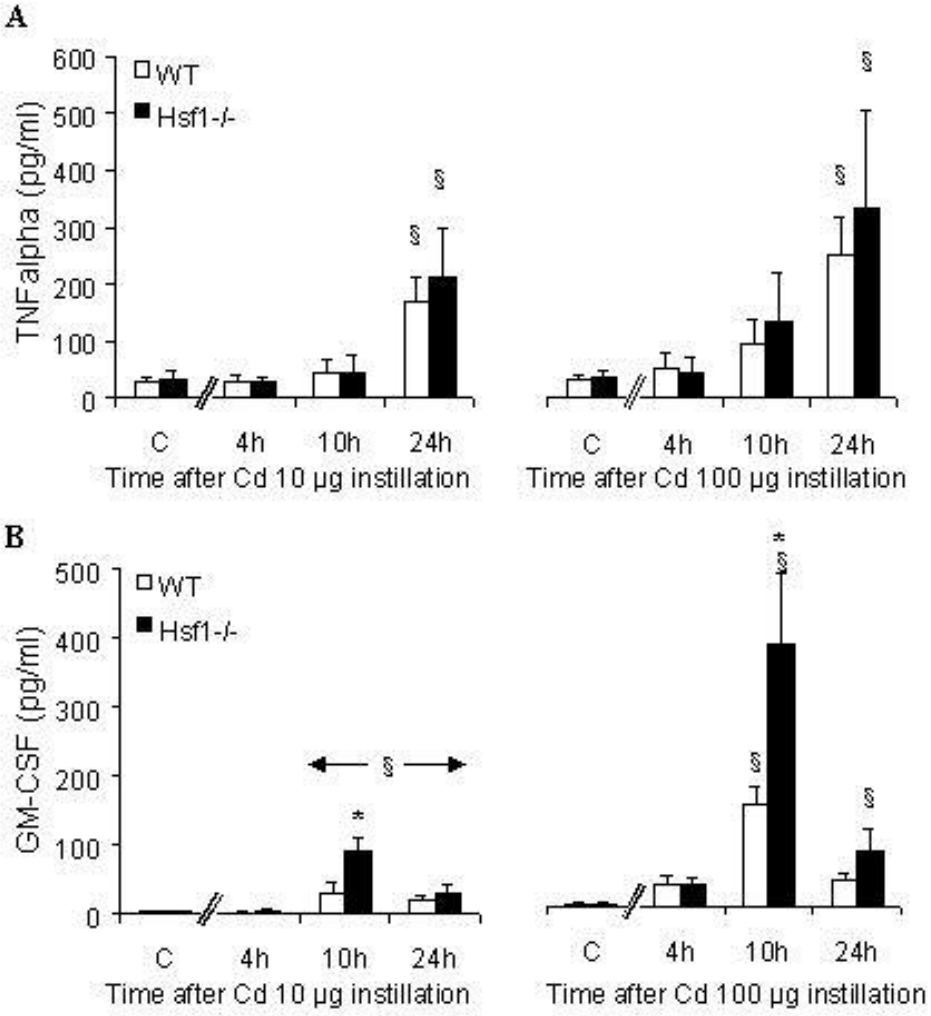
A
TNFalpha (pg/ml)
600
500
400
300
200
100
0
WT
Hsf1-/-
§
§
§
§
C
4h
10h
24h
Time after Cd 10 µg instillation
Time after Cd 100 µg instillation
B
GM-CSF (pg/ml)
500
400
300
200
100
0
WT
Hsf1-/-
§
*
*
§
§
§
C
4h
10h
24h
Time after Cd 10 µg instillation
Time after Cd 100 µg instillation

Figure 5

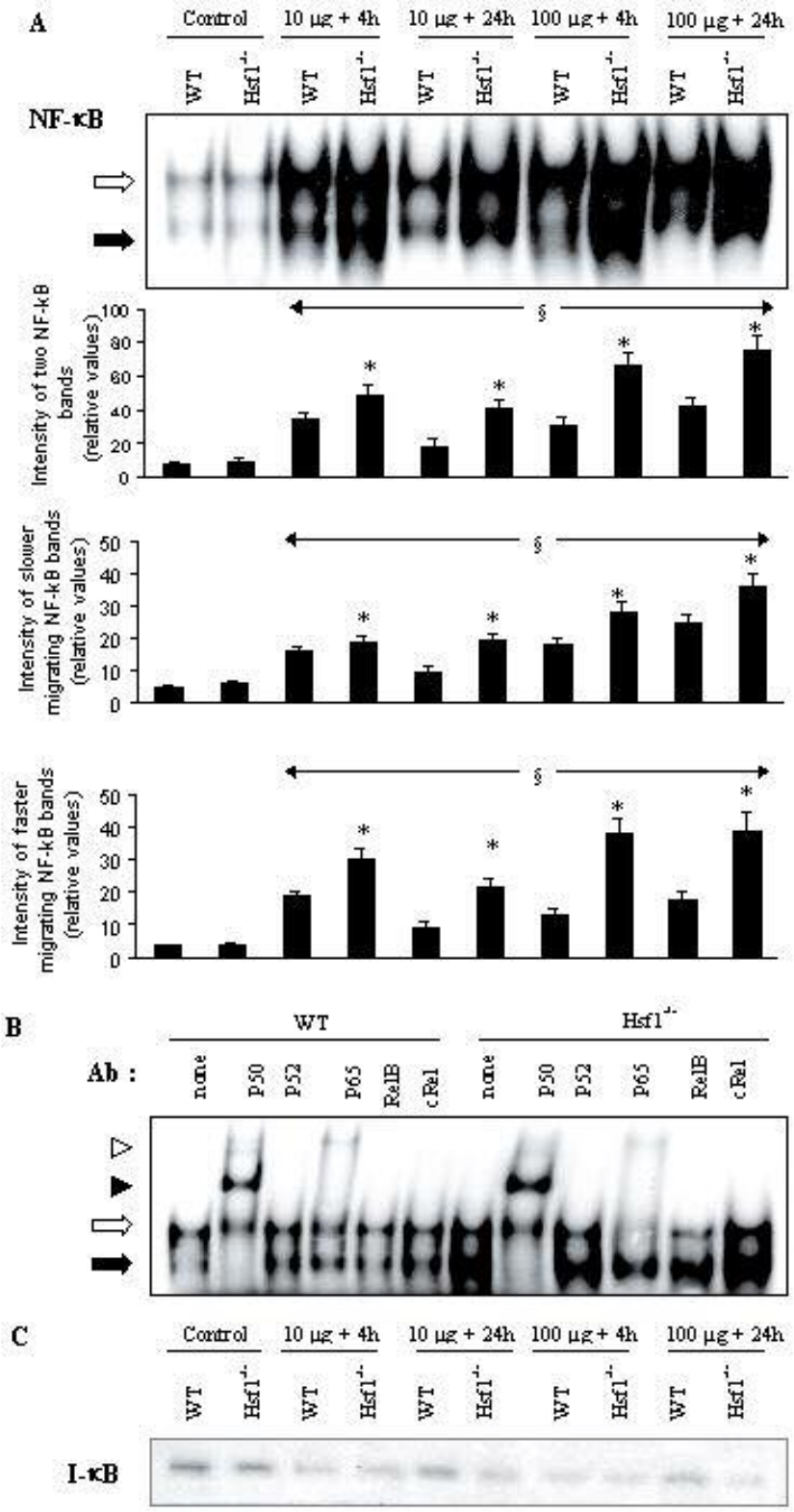
A
Control
10 μg + 4h
10 μg + 24h
100 μg + 4h
100 μg + 24h
WT
Hsf1-/-
NF-κB
Intensity of two NF-kB bands (relative values)
Intensity of slower migrating NF-kB bands (relative values)
Intensity of faster migrating NF-kB bands (relative values)
B
WT
Hsf1-/-
Ab :
none
P50
P52
P65
RelB
cRel
C
I-κB

Figure 6